539.107.4

RADIATION MEASUREMENTS IN SPACE

L. S. GORN and B. I. KHAZANOV

Usp. Fiz. Nauk 95, 353–381 (June, 1968)

THE launching of the first artificial Earth satellite in the Soviet Union in 1957 gave rise to a new field of science, space studies. Many scientists, including physicists, geophysicists, astronomers, and biologists have conducted intensive studies in satellites and space ships launched in the last decade. The number of experiments and their complexity and distance of flight have grown from year to year.

A considerable number of the performed studies have involved radiation measurements. These measurements are of independent interest (e.g., in cosmic-ray physics, geophysics, x-ray astronomy, radiation surveying of the Moon and the other planets, radiation monitoring of solar activity, and in dosimetry on cosmic objects, etc.). They are also used as a method of solving a number of other problems (e.g., for measuring the fuel level in tanks, determining the presence of life on other planets, and for material analysis of rocks on the surface of the Moon and the other planets, etc.). It is no wonder that one of the most important scientific results obtained in recent years, the discovery of the radiation belts around the Earth, involved radiation measurement in space, while monitoring of the ionizing-radiation parameters in a space ship is considered one of the most important conditions for ensuring safety of space flight.

Measurement of radiation in space is closely linked with invention of the necessary special apparatus. The peculiarities of the conditions of measurement have determined the specifics of these radiometric instruments, and have led to invention of many types of apparatus specialized for measurements under space conditions. As we know, a set of overall requirements is imposed on any apparatus put in space ships and artificial Earth satellites. They include smaller dimensions and weight of the instruments, lowered energy requirement, long service life, stability to mechanical effects (shock, vibration), and the possibility of thorough testing. Instruments located outside the hermetically-sealed compartment are subject to the extra requirements of stable operation over a wide temperature range, under high vacuum, etc.[1] This has made for invention of new methods of building apparatus, and for new solutions in circuitry and design.

Besides these general requirements, research apparatus is characterized by a number of features determined by the specifics of the object of measurement: flux magnitudes, energy distribution, and forms of radiation in space. This review is concerned with the design of this research radiometric apparatus.

1. CHARACTERISTICS OF RADIATION FLUXES IN SPACE

The measurements that have been made permit us now to draw an approximate picture of the radiation fluxes in space near the Earth and in interplanetary

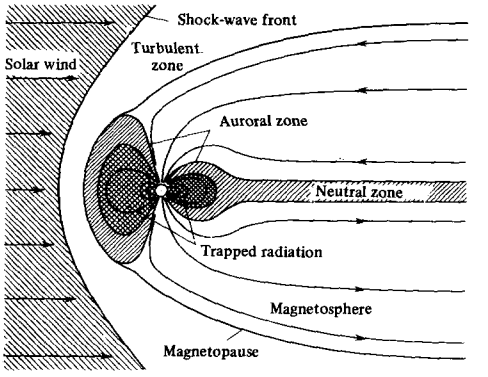

FIG. 1. Radiation distribution in space in the vicinity of the Earth.

space (Fig. 1), and to estimate the characteristics of the radiation to be studied further. The fundamental components of the ionizing radiation are: primary cosmic radiation, radiation captured in the geomagnetic trap, the solar wind, a complex of radiation effects occurring in chromospheric flares of the sun, and the auroral radiation. The greatest weight is put here on fluxes of charged particles, electrons and protons. Figures 2 and 3 give the flux densities of charged particles in different energy ranges for the different radiation components.

The solar wind is a flux of plasma ejected radially by the hot corona of the sun.[2-4] Near the Earth, it consists mainly of low-energy protons and electrons. The density of the plasma amounts to 0.5–30 particles/cm^3. Since the wind velocity is 300–800 km/sec (the latter value occurring at times of solar perturbations), this corresponds to flux densities of 1.5×10^7–2×10^9 particles/cm^2·sec. The proton fluxes of the solar

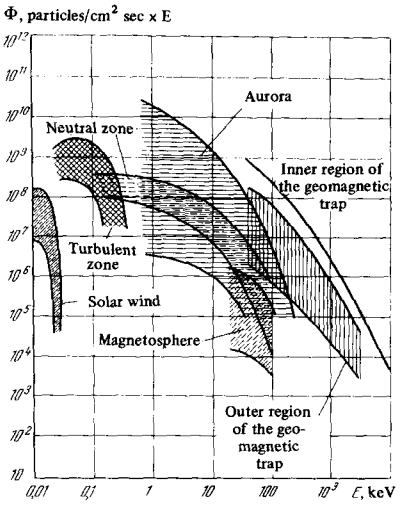

FIG. 2. Energy distribution of electron fluxes.

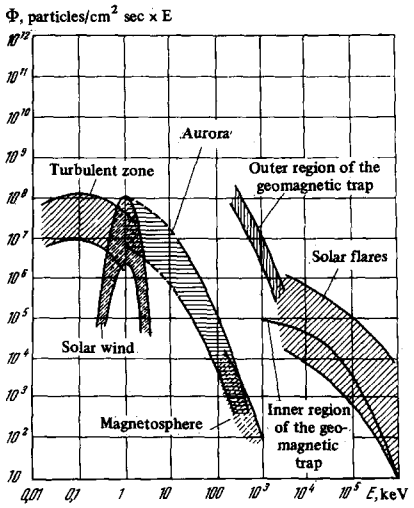

FIG. 3. Energy distribution of proton fluxes.

wind have a very narrow directional diagram (±12°). The electrons are distributed almost isotropically, since their thermal velocity component ($E'_e \cong 30$ eV) is considerably greater than the directional component ($E''_e \simeq 1$ eV). Sometimes electrons are found with energies of 0.1—1 keV, and rarely electrons are detected with $E > 40$ keV and protons with $E > 180$ keV.[5] The object of measurement in the solar wind is usually the time variation of the energy distribution of the particles, the electronic and ionic temperatures, and the particle concentrations.

The Earth and its surrounding magnetic field form the magnetosphere, a cavity bathed in the solar wind. A shock-wave front is formed at a distance of about 80,000 km as the solar wind collides with the geomagnetic field of the Earth. The geomagnetic field of the Earth is distorted, and a transition region, or turbulent zone, is formed between the shock-wave front and the edge of the magnetosphere.[4,6,7] Within it, the protons of the solar wind lose part of their energy, imparting it to the electrons of the plasma. However, they retain a considerable velocity component approximately lying along the boundary of the magnetosphere. The direction of motion of the protons becomes more chaotic, and the angular distribution less sharp (±60°). The energy of the electrons in the turbulent zone rises to values of ~1 keV. Sometimes a small fraction of the electrons is accelerated to energies considerably above 30 keV.

A region of particles caught in the geomagnetic trap is marked out within the magnetosphere.[3,4,8] The earthward boundary of this region is fixed by the atmosphere (on the average about 600 km from the Earth's surface). Protons of very high energies (up to hundreds of MeV) are trapped in the very strong magnetic field near the Earth. The stability of the magnetic field also makes for a considerable stability of the flux densities. As we go further from the surface of the Earth, the mean energy of the trapped protons decreases. At h = 10,000 km, it drops to fractions of an MeV, and flux-density fluctuations arise, and become as great as 30—100%.

The electron distribution in the trapping region has two maxima: one at about 2500 km above the Earth's surface, and the other at about 20,000 km (in the equatorial plane in a direction opposite the sun). The trapped particles show angular anisotropy. The angular distribution has the form of lobes perpendicular to the lines of force, with a wide spread in the equatorial plane, and narrowing as one moves along a line of force toward the Earth. Determination of the time variations of the flux density and the energy and angular distributions is one of the fundamental problems in measuring the trapped radiation.

Outside the trapping region, the magnetosphere is filled with a plasma of electrons and ions of energies 1—100 keV.[4-9] The Earth's magnetosphere has a long, almost cylindrical tail containing a magnetic field and the plasma arising from it. It is caused by entrainment of the lines of force by the solar wind. The equatorial region is a neutral layer in which the pressure of the surrounding magnetic field balances the increase in the plasma concentration. The electron flux density in this region varies considerably from measurement to measurement. At times, changes occur in the energy distribution of the particles, accompanied by decrease in the fraction of low-energy electrons and increase in that of high-energy electrons. In measurements of flux densities of electrons having energies above a given value, this is manifested as bursts of flux density (the so-called "electron islands"). Angular-distribution measurements have shown that in many cases electron fluxes having $E > 40$ keV move away from the sun in the region of the geomagnetic tail. This movement continues for up to several hours. The angular distribution of the low-energy electrons (0.3—20 keV) is usually isotropic.

The aurora, a phenomenon that is sporadic in nature, is due to intrusion into the atmosphere of charged particles: electrons and protons having energies from a fraction of a keV to hundreds of keV.[4,6,10] The electron beams are characterized by localization (the beam dimensions amount to several km, and sometimes to a fraction of a kilometer) and by considerable variability. The proton beams vary slowly, and they extend for hundreds of kilometers. The angular distribution of the electrons in the currents is almost isotropic, while the protons show no isotropy. The object of measurements of the auroral radiation is to detail the energy and angular distributions of the charged particles, and to determine their time variations.

Chromospheric flares on the sun give rise in interplanetary space to a flux of charged particles (90% proton and 10% α particles; some flares have shown heavier nuclei).[11,12] Little is known about the electron fluxes produced by solar flares. Solar flares are provisionally divided into two classes, A and B, depending on the intensity of the proton flux and their energy spectrum.

Fluxes of relativistic particles of solar origin arising from Class B flares are characterized by protons of energies up to 15—50 GeV having a directional angular distribution. The flux density becomes as high as 10^7 and sometimes even 10^8 $cm^{-2}sec^{-1}MeV^{-1}$. The latter values of the flux density are observed no oftener than once or twice a year in a period of solar activity. The flux rises for a short time (20—40 min) after the onset of the flare, and then declines with time like t^{-1} to t^{-2}.

The fluxes of non-relativistic particles occurring in Class A flares are considerably more frequent. They rise slowly (for up to several tens of hours), and decline for a time of as much as a hundred hours. The proton fluxes are weaker (up to $10-10^2$ $cm^{-2}sec^{-1}MeV^{-1}$), and their energy range is 10–500 MeV. The spectra become softer as the intensity of the flare declines. The particles in the fluxes produced in Class A flares are characterized by an isotropic angular dependence.

The primary cosmic radiation is a flux of charged particles (85% protons, 13–14% α particles, and 1–2% heavy nuclei of atomic numbers up to 26) of energies from several MeV to 10^{13} MeV and higher.[11] The flux density amounts to 2–2.5 particles/cm^2sec at a peak of solar activity, and it rises by a factor of 1.5–2 at minimum activity. The spectrum falls sharply with increasing energy: the flux density at energies above 10^4 MeV is about 0.1 particles/cm^2sec, and is about 10^{-6} particles/cm^2sec above 10^6 MeV. The angular distribution of the particles is isotropic (at least to within several percent).

In addition to fluxes of charged particles, other objects of measurement in space are electromagnetic radiation (X-rays and γ rays) and neutron fluxes.

The sun continuously emits soft x-rays. The differential energy spectrum of the quiet sun is rather soft, and the total energy flux for $E > 1$ keV amounts to about 6×10^4 keV/cm^2sec.[5] During solar flares the x-ray flux increases by several orders of magnitude, while the energy spectrum becomes harder (Fig. 4a).

Gamma quanta and neutrons in space fundamentally result from interaction of primary cosmic radiation with the upper layers of the atmosphere. Inelastic collision of the nucleons forming the primary component of the cosmic rays with the nuclei of atoms in the atmosphere gives rise to secondary particles of the first order. These include neutrons, mesons, hyperons, and nuclear fragments. The products of their decay or collision with nuclei of the atmosphere are second-order particles (including neutrons) and γ quanta.

About 10% of the neutrons formed interact with nuclei at high and intermediate velocities, and emerge from the atmosphere (albedo fluxes). The neutron fluxes (Fig. 4b) are characterized by a considerable latitude-dependence: above the pole the neutron density (at an altitude ~600 km) is $(1.1 \pm 0.2) \times 10^{-7}$ neutrons/cm^3. Above the equator the neutron density is an order of magnitude smaller.[13]

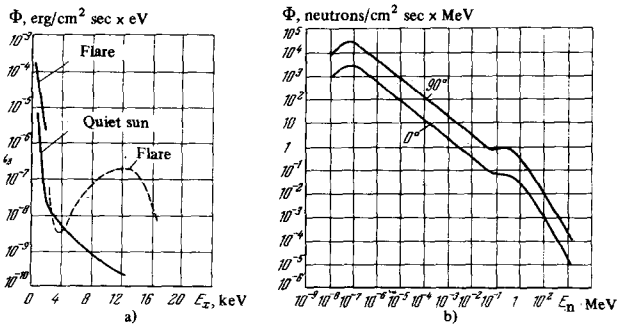

FIG. 4. Energy distribution of solar x-rays (a) and neutron fluxes (b).

Albedo neutrons and γ quanta result from interaction of cosmic rays with the Moon's surface. Thus, the flux density of secondary γ quanta in the vertical direction is estimated to be 0.5 kV/cm^2sec · sr at $E \geq 1$ MeV.[14] Finally, one of the components of the electromagnetic radiation is bremsstrahlung caused by interaction of electrons with the atmosphere. The total intensity of the bremsstrahlung involves the energy E_0 of the incident electron and the parameter Z of the medium by the amount 5.77 ZE_0^2 MeV/electron. That is, the probability of producing bremsstrahlung quanta increases considerably with increasing electron energy. The center of the spectral distribution of the bremsstrahlung is shifted toward smaller energies: 27% of the quanta have energies below 0.1 E_0, and 60% of the quanta below 0.3 E_0.

Measurements made on the space ships Ranger III and Ranger V have shown that the differential γ-ray spectrum at energies of 70 keV–4.4 MeV has the form $E^{-2.3}$ at a distance of $(70-400) \times 10^3$ km. The integral quantum flux is close to 3 kV/cm^2sec.[15]

The very brief discussion presented here of the fundamental characteristics of the different components of the radiation fluxes indicates the most characteristic problems of measurements in space. They include:

a) determining flux densities of radiation over a broad range of energies with a broad range of extreme values;

b) measuring radiation both in the very-low-energy range (from tens of eV to tens of keV), and in the region of considerable energies (up to 1000 MeV and above);

c) determining one of the types of radiation (electrons, protons, gamma, and neutron radiation) on a background of other components;

d) measurements of rapidly varying fluxes of small extent (the aurora).

Thus, the radiometric apparatus must have a wide dynamic range, flexibility in the data-collection and -transfer systems, and in a number of cases, little lag. Especially serious problems fall on the detection units, which must permit selective measurement of radiation of a given type and energy on a background of radiation of different types and energies over a range from extremely small to very high energies.

2. DETECTION OF PROTONS OF INTERMEDIATE AND HIGH ENERGIES

The lower limit of the energy range discussed in this section is determined by the thickness of the entrance window of the detectors needed to protect them securely from sunlight. When one uses the better light-shielding foils made of aluminum or nickel of thickness ~0.2 mg/cm^2, the lower limit of detectable energies amounts to about 100 keV.[9] The upper limit corresponds to relativistic protons of galactic origin, with energies of 10–100 GeV and above. Thus, the dynamic range of intermediate- and high-energy protons amounts to at least 10^5-10^6.

Charged-particle detectors are not yet known that can permit detection over such a broad range. Any actual detector is suitable for measuring energies only over a very limited energy range. Here protons of another energy range can produce false background readings. Other sources of background signals are

intermediate- and high-energy electrons, and also heavy-nuclei having $Z > 1$ of solar or galactic origin. Hence, high selectivity of the detectors is a fundamental condition for getting reliable information in the measurements being made. That is, they should show selective sensitivity to protons of the given energy range (outside of which it is close to zero), and insensitivity to electrons and heavy nuclei of all other energies (or at least reliable accounting for such a background).

In practice, the required selectivity of the detectors is attained by several methods that can be applied, depending on the conditions of measurement: the energy range of the protons being detected, their flux density, and also the flux density of the background particles and their spectrum. These methods include: using permanent magnets to intercept electron fluxes, building detectors with sensitivity thresholds, and finally, using composite detectors.

Elimination of the electron background by putting a permanent magnet at the entrance window of the detector is widely used in instruments for measuring proton fluxes.[16-19] One usually uses magnets of field intensities about 1000 Oe. The radius of revolution of electrons of energies less than 1 MeV in the field of such magnets is about a centimeter. This makes it possible to deflect them from the aperture window, and hence, to reduce the background considerably.

Detectors having sensitivity thresholds have been rather widely applied in practice, especially in the early experiments, i.e., detectors whose efficiency differs from zero only above a certain threshold energy.

A large group of threshold detectors comprises instruments consisting of a detector enclosed in an absorbing envelope. The thickness of the absorber determines the energy threshold of the detector. In practice, both proportional detectors[19,20] and non-proportional detectors (such as the Geiger counter)[21] have been used as the detecting elements in these instruments. Performing measurements with a set of threshold detectors differing in thickness permits one to get the integral spectrum of the particles. After data reduction (differentiation), one gets the differential spectral distribution. The merit of threshold-detector instruments is the simplicity of the detecting apparatus itself, and of the electronic circuitry. However, they have certain inherent defects, especially if one is using a non-proportional detecting element. This involves the fact that such a detector cannot distinguish protons from electrons nor from bremsstrahlung produced in the filter when irradiated by electrons. Hence, the results of such measurements often prove to be hard to decipher, and in the early experiments they were interpreted with considerable errors.[22]

Use of proportional detecting elements surrounded by absorbers permits one to increase the selectivity of the apparatus by a supplementary pulse-height analysis output signals, as has been done, e.g., in[18]. Semiconductor lithium-drifted detectors of a layer depth ~1 mm were surrounded by absorbers whose thicknesses corresponded to transmission of protons of energies 10, 20, 35, and 60 MeV, and electrons of energies 0.7, 1.4, 3.8, and 9.2 MeV, respectively. Since most of the electrons transmitted through the filter retained energies close to relativistic values (several hundreds of keV), their linear ionization losses amounted to ~2 keV/(mg/cm^2). This is almost three times as small as for 100-MeV protons. This permitted the authors to distinguish protons from electrons by a very simple pulse-height analysis. The threshold of the integral discriminator was set at about 1 MeV, whereas the energy deposited in the detector when detecting fast electrons was ~0.5 MeV.

Another group of threshold detectors consists of Cerenkov counters.[23,24] As we know, electromagnetic radiation is generated when a relativistic particle moves in a medium at a velocity greater than that of light in the same medium. Here the number of emitted photons per unit path traversed by the particle is[23]

$$\frac{dI}{dx} \cong 450Z^2\left(1-\frac{1}{n^2\beta^2}\right),$$

where n is the refractive index, $\beta = v/c$ is the ratio of the particle velocity to the velocity of light in vacuo, and Z is the charge of the particle.

The threshold velocity v_{thr} of the particle equals c/n. This corresponds to a threshold energy of protons $E_p^{thr} \cong 300$ MeV. The strong (quadratic) dependence of the signal on the charge makes it possible to distinguish the nuclear components of the galactic cosmic radiation, since when $v \simeq c$, the signal amplitude is determined only by Z^2. We must note that the threshold of Čerenkov counters for electrons is $E_e^{thr} \cong 0.2$ MeV. Hence, protons can be measured either outside the trapped-radiation zone, or by using shields that completely absorb the electron component.

In a number of studies of proton fluxes of intermediate and high energies, high selectivity of the apparatus was attained by using composite detectors containing at least two sensitive volumes.[17,18,25-29] The purpose of using a composite detector is usually to eliminate the ambiguity of the pulse response of the detector in detecting soft and hard protons.

One can grasp the essence of this ambiguity by examining the family of curves (Fig. 5) showing the relation of the energy deposit ΔE in detectors of differing thicknesses to the energy E_p of an incident proton. The values of the detector thickness, as a parameter of the family, are plotted on the diagonal straight line, which forms the initial region of all the curves up to the value $E = \Delta E(\delta)$. The left-hand portion of each curve corresponds to total loss of the energy of the particle in the

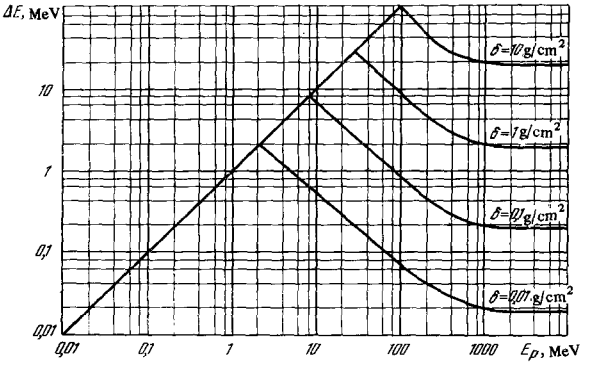

FIG. 5. Energy deposit ΔE made by protons in the detector material as a function of the detector thickness δ and the proton energy E_p.

detector, while the right-hand portion corresponds to an interaction in which the range R of the particle exceeds the thickness δ of the detector. When $R \gg \delta$, the energy deposit is proportional to the linear energy loss dE/dx. We see from the curves that one value of the energy deposit ΔE can correspond to two values of the particle energy. This makes the response of the detector ambiguous. Hence, in designing composite detectors, one tries to build them to select cases of total energy loss (E measurement) or cases of linear energy loss, from among all the possible events of interaction of particles with the detector. The amplitude spectrum of the signals obtained in E measurements directly corresponds to the energy distribution of the particles. A signal spectrum proportional to the linear losses can be recalculated to give the energy distribution by using the mutually unequivocal functional relationship $dE/dx = f(E_p)$.

One usually realizes the E-measurement case by designing the detector so that its main sensitive volume (in which the energy deposit is measured) is surrounded by an auxiliary detecting shield, while the electronic logic circuits select only those events in which the signal from the main detector is not accompanied by firing of the shielding circuit.

In dE/dx measurements, the detection unit is constructed like a telescope made of two or more detectors connected for coincidence so that the energy deposit in the first detector is measured whenever accompanied by simultaneous firing of the second one.

Composite E detectors are usually used in measuring energy spectra of protons in the range from ~100 keV to several tens of MeV. As we have noted, the lower limit is fixed by the thickness of the light-shielding entrance window, while the upper limit is fixed by the practical depth of the sensitive volume of the detector (of the order of 3–5 g/cm^2). Figure 6 shows the construction of a typical composite detector of this type.[18] The basis of the detector is a scintillation counter whose constituent phosphor element is a single crystal of CsI(Tl). Except for the plane of incidence of the particles, it is surrounded on all sides by a container made of a scintillating plastic. To reduce the counting rate and to provide a sharply-defined directional diagram, the phosphor is enclosed in an absorber about 5 g/cm^2 thick, which absorbs protons of energies up to 70 MeV and electrons up to 10 MeV. Electrons softer than 1 MeV are eliminated with a permanent magnet placed in front of the entrance aperture.

Two modifications of the detectors are cited in this study. One of them, intended for measuring proton fluxes in the range 0.1–4 MeV, has a CsI(Tl) crystal of thickness about 50 mg/cm^2. Relativistic electrons deposit less than 0.1 MeV of energy in such a crystal, and thus they are not recorded.

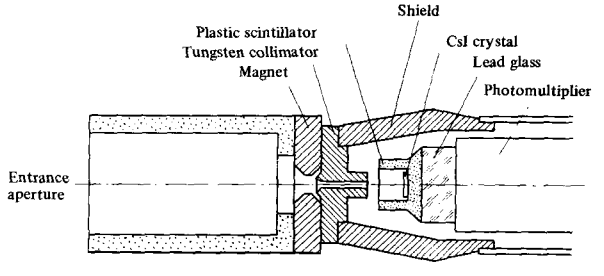

FIG. 6. Design of a detector for intermediate-energy protons.

The second detector modification has a thick CsI(Tl) crystal of thickness 10 g/cm^2. It is intended for recording protons over the energy range 4–100 MeV, but is not shielded from electrons of energies 4–20 MeV. With this counter design, one can eliminate electrons by limiting the energies of recorded protons to the range 4–30 MeV. Here it would seem possible to reduce the thickness of the CsI(Tl) crystal to ~1 g/cm^2. In such a crystal, the energy deposit in detecting relativistic electrons with an appreciable probability is less than 4 MeV. In both designs, particles having R greater than the thickness of the CsI(Tl) crystal cause scintillation in the surrounding plastic scintillator, and are rejected by a shape-discriminator circuit.

The distinction of signals arising from scintillations in the plastic scintillator or in the CsI(Tl) crystal is based on the difference in emission times τ. Thus, $\tau < 10^{-8}$ sec for the plastic, while $\tau \cong 0.7 \times 10^{-6}$ for the plastic. The emission time determines the duration of the current pulse arising at the photomultiplier output. The shape discriminator separates the current pulses into two components. The presence of a signal having a fast component in the current pulse indicates scintillation in the plastic, while a signal having a slow current component indicates scintillation in the CsI(Tl) crystal.

A refined composite detector for fast protons is described in[17]. In it, relativistic particles in the range 10–100 MeV (including electrons) are discriminated with a supplementary scintillation counter containing a thin CsI(Tl) crystal at the entrance of the system. This counter forms a telescope together with the second counter, which is provided with a phoswich. Relativistic particles are discriminated by pulse-height analysis of the signals from the first counter, which measures the linear losses dE/dx of the incident particles. The counter is analogous in other respects to that discussed above.

When studying spectral distributions of protons of energy above ~100 MeV, the method of measuring energies by determining ranges requires detectors that are too "thick". Thus, the required detector thickness for spectrometry of protons of energies up to 200 MeV is about 30 g/cm^2. Hence, in the near-relativistic range one prefers methods for spectrometric measurements that are based on measuring linear loss (dE/dx) spectra.

The composite detector in a linear-loss spectrometer is made in the form of a telescope consisting of two or more detecting elements.

The data-processing electronic circuit selects only the signals from the first dE/dx detector that are accompanied by a simultaneous signal from the second detector. The thickness of the dE/dx detector is chosen such that the hardest particles in the range being detected deposit an energy in it sufficient for reliable pulse-height analysis measurement over the noise level of the apparatus. Thus, e.g., in building a dE/dx spectrometer for protons with an upper limiting energy of ~1 GeV and higher, based on a semiconductor detector, the thick-

ness of the depleted layer must be about 0.1 g/cm^2. A relativistic particle deposits an energy of ~200 keV in such a detector. This is about an order of magnitude higher than the noise level of the transistor preamplifiers used to amplify the pulse signals at the output of the detectors. Sometimes the telescope is made more complex by increasing the number of detectors and inserting absorbers of definite thicknesses between them in order to obtain more complete information.

As an example, Fig. 7a shows a schematic diagram of a telescopic composite detector intended for separate measurement of fluxes of galactic protons and α particles in the energy range 1–170 MeV/nucleon, as well as α particles of energies above 170 MeV.[26] It consists of three surface-barrier silicon detectors D_1, D_2, and D_3 enclosed in a cylindrical case. An absorber of thickness about 50 mg/cm^2 is put between the detectors D_1 and D_2 to stop particles of energies below 15 MeV/nucleon. Between D_2 and D_3 is an absorber of thickness ~5 g/cm^2, which transmits particles of energy about 70 MeV/nucleon. The measuring circuit sorts the pulses from detector D_1 into three groups corresponding to the following events:

1) firing of D_1 with no signal at the output of D_2;
2) firing of D_1 and D_2 but no signal from D_3;
3) firing of all three detectors;

Figure 7b shows the relation of the energy losses in the detector D_1 to the energy of incident particles for protons and α particles, and indicates which of the three listed groups of events these loss values pertain to. We see that the absorbers divide the energy-loss curve into three regions: 1–15 MeV/nucleon, 15–70 MeV/nucleon, and 70 → ∞ MeV/nucleon. Pulses in the first zone are due to either protons or α particles of energies 1–15 MeV. We see from the graph that we can distinguish protons from α particles if we set the discriminator threshold at ~3 MeV. In the second zone, the linear energy-loss spectrum of protons extending from 0.5 to 2 MeV is distinct from the linear loss spectrum of α particles having limits of 2–8 MeV. This permits us to record them separately. Finally, in the third zone, we can completely discriminate hard protons from α particles of energies >170 MeV/nucleon by a suitable choice of the threshold (~0.3 MeV). The cited groups of events are distinguished in the instrument by a special logic circuit.

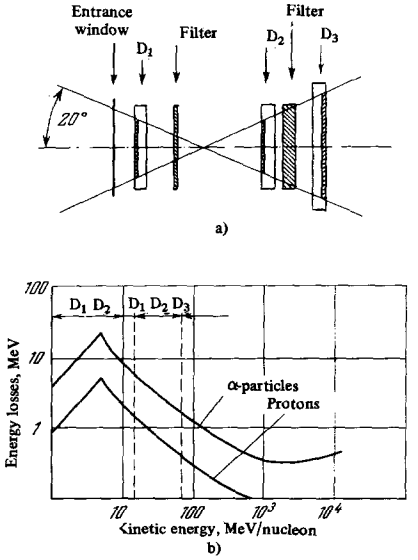

FIG. 7. Arrangement of detectors in a telescope (a), and a graph of the energy losses of protons and α-particles in the detector D_1 (b).

Another variety of telescopic detectors intended for analysis of heavy charged particles in terms of charges and masses consists in the so-called (dE/dx) × E composite detectors.[30,31] These detectors consists of two detecting elements. The first is of small thickness, and measures the linear energy losses. The second has a thickness exceeding the range of the hardest particles in the energy range being analyzed. Thus the signals at the output of the first detector are proportional to the linear ionization losses, while those at the output of the second detector are proportional to the energy of the particles stopped in it. The physical possibility of sorting particles by using such a detector is based on the idea that the product of dE/dx by E in the subrelativistic energy region depends to a first order of approximation only on the charge of the particles and their masses:

$$\frac{dE}{dx}E = 0{,}075q^2Mc^2 \ln\left(\frac{1{,}6\cdot 10^5}{Z}\frac{E}{Mc^2}\right) = f(q^2, M)$$
$$\left(\text{when } \frac{E}{Mc^2} \ll 1\right).$$

In this expression, dE/dx is in MeV/(g/cm^2), E (in MeV) is the kinetic energy, Mc^2 (in MeV) is the energy corresponding to the rest mass, q is the charge of the particle, and Z is the atomic number of the detecting medium.

In actual instruments, the signals at the outputs of the two detectors are logarithmized with analog logarithmic devices, and are then added.[31] Thus, the overall signal is proportional to the logarithm of the product (dE/dx) E, and the problem of analyzing particles in terms of charges and masses is reduced to ordinary pulse-height analysis.

The material that we have presented permits us to make a comparative evaluation of the discussed methods of selective detection of protons in different energy groups.

Threshold detectors containing absorbing filters are rather universal in the proton energy range from 0.1 to ~100 MeV. The upper limit of this range corresponds to a filter thickness of ~10 g/cm^2. Hence, it is not suitable to extend this method to particles of higher energies, in view of the considerable increase in the weight of the filter. It is preferable to use proportional detecting elements in these detectors, since this makes it possible to reject relativistic particles and γ quanta by pulse-height analysis. Further, we must recognize that threshold absorbing detectors have the defect that one can't get the differential distribution with one detector, and that the information obtainable with them is thereby limited.

Use of composite detectors provides for obtaining more reliable (with respect to simplicity and unambiguous interpretation) and complete information. Here, as it seems, the best selectivity is attained by dividing the entire range being detected into four intervals covered by the appropriate detectors.

For detection within the first interval from 0.1 to ~3 MeV, it is convenient to use a composite E detector with a thickness of the fundamental detecting sensitive volume (scintillator or semiconductor) of about 20 mg/cm^2, shielded from penetrating particles by a detecting shield. Pulses arising from electrons are reliably suppressed by this choice of detector thickness and by setting the threshold of the analyzing circuit at ~100 keV. Hence, in this detector one need not use a magnet to keep out electrons. However, if the instrument is designed to operate in the presence of considerable electron fluxes, in line with the conditions of measurement, installing a magnet is a useful measure that considerably simplifies the conditions of operation of the analyzing circuit. For the same purpose, one can shield the detecting element (except for the aperture window) with an absorber ~ 5 g/cm^2 thick to eliminate the soft component of the cosmic radiation.

Protons of the next energy interval, which extends from 3 to ~30 MeV, can also be conveniently detected with a composite E detector of thickness ~1 g/cm^2. With this detector thickness, the energy deposited when detecting electrons is less than 3 MeV, and electrons can be rejected by pulse-height analysis.

Protons in the next, pre-relativistic interval 30—300 MeV can be conveniently detected by using a dE/dx telescopic composite detector having a main detecting element about 200 mg/cm^2 thick. The corresponding range of linear energy losses is 15—3 MeV/(mg/cm^2), and the range of energies deposited by protons in the detector is 3—0.6 MeV. As before, relativistic protons and electrons can be rejected by pulse-height analysis.

Finally, relativistic protons of energies above 300 MeV in the last interval can be detected most conveniently, as was mentioned above, by Čerenkov counters. Using them permits one to eliminate the background of all protons of energies below the threshold, and also to accomplish charge selection. Electrons can be rejected by shielding the detector with an absorber whose thickness suffices to absorb the hardest background electrons.

3. DETECTION OF INTERMEDIATE AND HIGH-ENERGY ELECTRONS

The limitations arising from the light-protecting foils and from noise in the detecting elements and the front-end amplification stages fix the lower limit of the range under discussion at a level of ~10 keV.[19] The upper limit of this range corresponds to the hard trapped-radiation electrons of energies ~5 MeV.

In principle, one can use the same detectors to detect electrons of these energies as are used in studying proton fluxes. However, in making them, one usually takes into account the peculiarities of the mechanism of interaction of electrons with the detecting medium. Thus, for example, in view of the considerable scattering of electrons, the concept of range becomes considerably less definite for them. Therefore, threshold detectors containing absorbers give less precise results when detecting electrons. In designing proportional detectors, one starts with the fact that the ranges of hard electrons are considerably shorter than for relativistic protons (of the order of several g/cm^2), and E-type detectors are granted preference. One uses two specific properties of electron fluxes to gain high selectivity of the detectors: their relative ease of deflection in a magnetic field, and also their smaller mean density of ionization energy losses, since the "center of gravity" of the electron spectrum to be studied is shifted into the relativistic region (as compared with the proton spectrum).

Using magnets in electron detectors solves a problem opposite to that which they solve in proton detectors.

While the magnet deflects electrons away from the detector aperture in proton detectors, its role in detecting electrons amounts to guiding the electrons to the detecting element. As a rule, the latter is located outside the field of view of the aperture window within the absorber. In practice, one finds two variants of design of electron detectors having magnetic "guidance."

In the first of these,[22,19] the detecting elements used are devices having a non-proportional reaction. In a detector designed for electron spectrometry in the energy range from 22 to 113 keV,[19] the detecting elements are four Anton-222 end-window Geiger counters, shielded on all sides (except for the entrance window) with a lead absorber of thickness ~3 g/cm^2. The electron flux transmitted by the entrance collimator enters the region of the field of a permanent magnet. The latter deflects the electrons of varying magnetic hardnesses and guides them to one of the counters, depending on their energy. Thus, all of the range being studied is divided into four energy intervals by the deflecting magnet and the four counters. However, we must acknowledge a defect of these detectors in that they can't distinguish the background due to penetrating particles. This difficulty has been overcome by introducing an additional counter shielded by an absorber on all sides including the window, to serve to monitor the background of penetrating particles.

The second variant of a magnetic-guidance detector includes instruments having proportional-type detecting elements.[17,18] An important advantage of using them is that one can then apply pulse-height analysis, and thus improve the selectivity of the detector. In these detectors, as in those discussed above, the detecting element (e.g., a scintillation-counter phosphor) is shifted off the collimator axis, and is located at some angle to it. This prevents protons from passing through the collimator to the detecting element. Figure 8 shows a typical design of a spectrometric detector intended for recording electrons in the energy range 50—1000 keV. In order to reduce the background of hard electrons and intermediate-energy protons, the scintillator (~0.5 g/cm^2) is surrounded by an absorber of thickness ~10 g/cm^2. As is usual in such designs, a light guide made of lead glass plays the role of absorber on the photomultiplier side. Penetrating protons are rejected by pulse-height analysis of the signals at the counter output. The possibility of rejecting them is based on the fact that the energy deposit in a crystal ~0.5 g/cm^2 thick exceeds 1 MeV in most cases when recording penetrating protons, since the probability is small that a proton should penetrate a 10-g/cm^2 absorber and deposit an energy <1 MeV in the scintillator, while the energy deposit in recording fast protons (up to relativis-

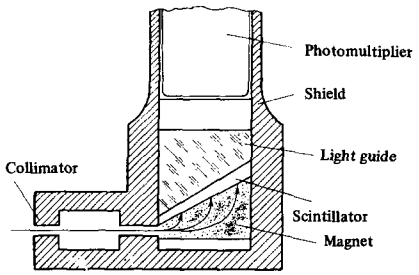

FIG. 8. Design of an electron detector.

tic velocities) exceeds 1 MeV.

Another method of rejecting penetrating particles in detectors of this design is based on using composite detecting elements.[18] In the instrument described in this study, a cesium iodide crystal is used as the scintillator to detect electrons. A plastic scintillator is set between this crystal and the light guide to reject penetrating particles. With use of the plastic scintillator, a shape-discriminator circuit rejects cases of dE/dx interaction of particles with the cesium iodide crystal. The range of electron energies recordable by this detector is 0.1–4 MeV.

We see from the above discussion that instruments using magnetic guidance of electrons to a proportional detector concealed in an absorber satisfy to the fullest degree the problem of measuring electron fluxes in space. Here we should make a remark. Since the range to be studied, 10–5000 keV, is rather broad, certain technical difficulties arise in building the electronic measuring instruments to permit pulse-height analysis over such a broad range. Hence it seems reasonable to overlap it with two detectors. The detector of the soft part of the spectrum from 10 to ~200 keV should be made with a thickness of entrance window of ~0.5 mg/cm^2 and a thickness of the detecting element of ~100 mg/cm^2. Further, the noise in the detector, and also in the front end of the amplifier should be low enough. One can use one of the detectors discussed above, with pulse-height or phoswich rejection of penetrating particles, as a detector of electrons of energies from 0.1 to 5 MeV. We should also note that Čerenkov counters can be successfully used for electrons of energies above ~200 keV.[29] Using them makes it possible to reject electrons of energies below 200 keV and protons of energies below 300 MeV.

4. DETECTION OF LOW-ENERGY CHARGED PARTICLES

In detecting low-energy charged-particle fluxes in the range from 10–15 keV down to tens of eV, the problems of selective recording are relatively simple to solve. Indeed, the effect of the high-energy charged particles passing through the structural elements of the detectors is not very substantial, owing to the considerable size of the flux densities involved. The fundamental problem in recording low-energy particles becomes that of shielding from the background arising from the visible and ultraviolet radiation of the sun.

Owing to the small penetrating power of electrons and protons of energies below 10 keV, these particles can't penetrate even quite thin foils (e.g., the ranges of electrons having E ≃ 10 keV and protons having E ≃ 100 keV are respectively 0.45 mg/cm^2 and 0.2 mg/cm^2 in aluminum). Hence, instruments to measure low-energy charged-particle fluxes must include an open (unshielded) detector. However, the intense visible and ultraviolet radiation of the sun acts on the surface of such a detector when unshielded from the environment. By existing estimates,[32] the electron emission when outside the Earth's atmosphere from a metallic surface having a low work function produces a current of the order of 10^{-8} A/cm^2, i.e., one equivalent to the action of a proton flux of density about 10^{11} particles/cm^{2}sec.

Since in the low-energy region the detector usually measures merely the flux of incident particles, one has to put devices in front of the detector to sort out the charged particles in terms of energy in order to carry out the energy selection. Two fundamental types of such devices are used in apparatus, based on selection by a stopping field.

In the detection units having a stopping field, a grid is placed in front of the detector (which is a charged-particle collector in the simplest case). A potential V_{grid} with respect to the collector is applied to the grid to retard the incident particles. Only particles having an energy E_{thr} sufficient to overcome the stopping field strike the collector. By varying the analyzing potential V_{grid}, one can measure the integral energy distribution of the electrons or ions in stages. It is characteristic of such detection units that one can attain a high sensitivity, which is proportional to the area of the entrance window.

The considerable current in the collector circuit due to photoelectric emission has practically ruled out the use of diode traps. A suppressor grid is introduced between the retarding grid and the collector in order to reduce this current, and a negative potential with respect to the collector is applied to it. Thus, photoelectrons emitted from the collector with energies less than the potential of this grid are stopped and return to the collector. Figure 9a shows a diagram of such a detector.[33,34] The photoelectrons emitted from the suppressor grid are partially collected by the collector, and give rise to an additional parasitic current component. However, the absolute value of this current component is cut down, both by incomplete reflection of ultraviolet light by the collector, and by the considerably smaller effective surface of the grid (the reduction in the cur-

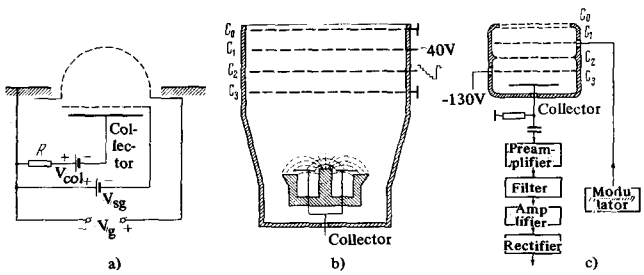

FIG. 9. Diagram of a detector using a stopping field and a suppressor grid (a), having the collector located in a magnetic field (b), and with modulation of the stopping field (c).

rent is as much as two orders of magnitude or more).

When one is measuring protons, the flux of secondary electrons and photoelectrons from the collector is considerably reduced if the collector is placed in a magnetic field. Then the radius of the trajectory of the ejected electrons, which mostly have small energies, proves to be much smaller than the geometric dimensions of the collector. Figure 9b shows a diagram of such a detector.[35,36] The ring collector is located in a magnetic field (~200 Gauss) whose lines of force are convex in shape at the surface of the collector. The secondary electrons, which have little energy, as a rule, move along the lines of force and return to the collector. It has thus been possible to reduce the photocurrent by four orders of magnitude, and thus a sensitivity of measurement was obtained of about 10^6 particles/cm^2sec, even when the detector was pointed at the sun. However, we should note that putting the collector in a magnetic field is applicable only for proton detectors. When low-energy electrons are being detected, the magnetic field greatly affects their trajectories.

In order to combat the interference due to secondary emission and photoemission, one can modulate the particle flux, and then measure the current in the detector circuit with a narrow-band amplifier.[37-39] Figure 9c shows the design of such an instrument, intended for measuring proton flux densities. The voltage on the grid C_1 is varied alternately from zero to the value V_{max} at the frequency f. Protons of all energies entering the trap strike the collector when the voltage is zero, while particles of energy below $E_{lim} = eV_{max}$ are stopped when the voltage is V_{max}, but the rest of the protons strike the collector. Thus an alternating current component arises in the collector circuit, proportional in size to the flux of particles in the energy range $O-E_{lim}$ (when the flux is normal to the plane of the grid). This current is amplified by a band amplifier and rectified by a synchronous detector.

In such instruments, it is important to eliminate coupling between the grid C_1 and the collector, which would give rise to parasitic signals. To do this, one introduces an additional grounded grid C_2 (or several grids) of reduced transparency. In addition, the grid C_2 reduces the effect of the modulating voltage on the size of the photocurrent from the suppressor grid to the collector, which is also one of the sources of errors. In such detectors, which have been used, e.g., on the satellite Explorer XI, the range of fluxes to be measured amounted to $4 \times 10^6 - 2 \times 10^{10}$ protons/cm^2sec, with an effective detector area of 18 cm^2 (the weight of the detector was 1.2 kg).[38]

The detection units for cosmic studies, having a deflecting field in the apparatus, include electrostatic and electromagnetic analyzers.

An electrostatic analyzer (Fig. 10) contains two cylindrical or hemispherical electrodes, between which a practically radial electrostatic field is formed. Particles of energies close to eV(R/2d) pass through the deflecting system and strike the collector.[40-45] The particles are focused after being deflected by 180° in the spherical analyzer, or 127° in the cylindrical analyzer. Most often, the energy resolution amounts to 5–20%. The angular diagram usually amounts to several degrees

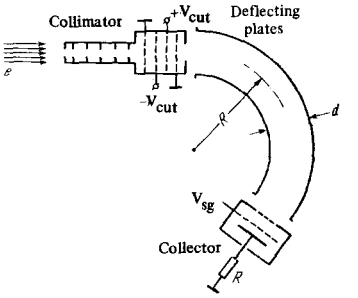

FIG. 10. Diagram of a detector using a deflecting electric field.

in the direction of the electric field, and 30–90° perpendicular to this direction. The geometric factor for such an analyzer amounts to 0.202 R^2 when d/R = 0.1.[46] Thus, for example, the analyzer used on the satellite Explorer XII had an angle of view 10° × 80°, and a flux of 10^6 particles/cm^2sec corresponded to a current of 10^{-13} A.[41] The electrostatic analyzer on the space ship Mariner II had an angle of view 20° × 20°, the area of the entrance window was 5 cm^2, and the resolution was $\Delta E/E = 0.25$; the collector current was measured over the range $10^{-13}-10^{-6}$ A.[47] In the spherical analyzers used on the satellites Cosmos 12 and Cosmos 15, $\Delta E/E$ amounted to 0.3, while the minimum detectable flux was 6×10^6 particles/cm^2sec · keV.[42]

In analyzers having a variable magnetic field, the particles pass through the gap of an electromagnet. The magnetizing current is varied to give stepwise variation of the magnetic field and of the energy value of particles passed by the deflecting system. Selectors were used in the apparatus, both with a homogeneous magnetic field, and with an inhomogeneous deflecting field and double focusing.[48] In the latter case, the magnetic field varies with the radius as $1/\sqrt{R}$, and the particles are focused after being deflected by $\pi/\sqrt{2}$ radians (about 255°). This system makes it possible to attain a considerably greater geometric factor than in instruments having a homogeneous field (0.02 sr · cm^2).

Analyzers using a deflecting field have a number of substantial advantages over detection units having a stopping field. First of all, this involves the diminished effect of visible and ultraviolet radiation on the collector. Multiple reflection of the ultraviolet radiation along the curvilinear trajectory of the particles reduces its intensity by several orders of magnitude. Furthermore, analyzers using a deflecting field permit one to get the differential energy distribution directly. The deflecting voltage in electrostatic instruments is less by a factor of R/2d than in those using a stopping field. This permits simplified design of the apparatus (usually the electrode voltages are equal in magnitude and opposite in sign).

The range of energies to be measured in the described magnetic analyzers lay in the range from units to several tens of keV. Here the maximum magnetizing current was 0.2 A. Electrostatic analyzers prove to be more economical; they can be made smaller and lighter (an instrument of this type described in[49] weighed less than 0.5 kg). The geometric factor of electrostatic analyzers is greater than in instruments having a magnetic deflecting field; the electric field is easier to monitor while scanning.

Thus, an electrostatic analyzer proves to be preferable for measuring fluxes of low-energy particles in space. The only exceptions are in measuring weak particle fluxes in the shadowed region, where it is advantageous to use stopping-field detectors. For detectors of both types, we must emphasize that one has to increase the work function of the surfaces of the collectors, deflection plates, grids, and other elements of low-energy particle detectors exposed to solar radiation in order to reduce the background level arising from the action of the visible and ultraviolet radiation of the sun. This property must persist for long periods under the conditions of operation of a satellite in the upper atmosphere.

In a number of instruments, electron or proton collectors have been used as detectors of the particle flux passed by the stopping field or the deflection system. In this case, the sensitivity of the apparatus is limited by the minimum current that can be measured by the electrometric amplifiers. For the minimum fluxes that are of interest, the current in the detector circuit is about 10^{-14} A, and the geometric factor (effective area) is made as large as possible. When one has to provide for satisfactory time characteristics of the detector, the current threshold measurable by the electrometric amplifiers is raised. Therefore people have begun to use in apparatus detectors of the discrete type: scintillation counters, open electron multipliers, and channel multipliers.

Using scintillation counters for low-energy particles involves the technique of post-acceleration. The particles passed by the deflecting system or the stopping field are accelerated by an additional electrostatic field, and gain an energy sufficient to pass through a thin foil and give rise to detectable scintillations in the counter crystal.

An example of such an instrument is an electron indicator containing a fluorescent screen (several mg/cm^2 of zinc sulfide or strontium phosphate coated on a plate set in front of a photomultiplier[35,50]. The current in the anode circuit of the photomultiplier is proportional to the energy flux of the electrons imparted to the scintillator. For protection from ultraviolet and visible light, the detector was covered with aluminum foil 0.4 to 1 mg/cm^2 thick. Three detectors having foils of different thicknesses (0.4, 0.6, and 1.1 mg/cm^2) were used to determine the energy distribution of the electrons, while the accelerating potential was raised in four steps from 0 to 4.3 kV (on the Cosmos 3) or to 11 kV (on the Cosmos 5). This permitted a series of measurements of the energy spectrum with twelve variants of the sensitivity curve. The course of the energy spectrum was determined by calculation. Thus they could attain a sensitivity to electrons of energies > 40 eV down to 10^7 particles/cm^2sec · sr. However, the energy resolution of this apparatus is rather low.

One can count directly the number of electrons passing through the deflecting system by using scintillation counters containing monocrystalline phosphors.[44,51] Then the accelerating potential must exceed 10 kV.

As compared with soft electrons, protons of the same energy have considerably shorter ranges, and an accelerating potential of hundreds of kV is required to make them pass through a foil 0.2—0.4 mg/cm^2 thick. Hence, proton detectors of this type have not been used in practice (except for Sharp's detector, which used a very thin foil (20 $\mu g/cm^2$) that did not protect the detector from light). However, systems have been described for measuring heavy charged particles, using emission of secondary electrons from the collector when struck by ions; the electrons are accelerated, and the accelerated electrons are detected by a scintillation counter.[52,53]

One can use "open" discrete detectors in apparatus for counting the number of low-energy (soft) particles: secondary-electron multipliers and channel multipliers. Mention has recently been made in the literature[5,44,53] on the use of open secondary-electron multipliers having dynodes made of beryllium-copper alloy. These multipliers permit one directly to count the number of electrons or protons passing through the entrance window. The area of the window amounts to several cm^2. In order to narrow the dynamic energy range of the electrons entering the secondary-electron multiplier, an increment of ~100 eV is added to their original energy by an accelerating field.[54]

Channel multipliers[54,55] are capillaries of inside diameter about 1 mm, several cm long. Their inside surface is covered by a semiconducting material having an overall resistance of $\sim 10^8$ ohms. When a high voltage (~3 kV) is applied to the end points of the capillary, the instrument works like a Geiger counter, generating an avalanche multiplication of primary charges that have been produced.

Furthermore, as is the case with scintillation counters having very thin foils, secondary-electron multipliers and channel multipliers are characteristically very sensitive to the ultraviolet and visible radiation of the sun and the aurora, and also to the reflected light of the daytime sky. Hence, one can use them only in conjunction with deflecting systems that substantially diminish the incident light. Here the collimation of the beam is not the limiting factor. Even when the effective area of the entrance window is 1 mm^2, a flux density of 10^5 particles/cm^2sec corresponds to a rate of pulse counting at the detector output of 10^3 pulses/sec. However, modulation of the analyzing voltage and difference-signal detection have been used even in systems containing discrete detectors in order to reduce the effect of ultraviolet radiation.

We see from the discussion above that discrete detectors are the most promising for detecting particles that have passed through selective devices. In addition, the small dimensions of channel multipliers permit one to make a parallel analysis of the energy distribution by arranging them in a row and deflecting the electrons by the field of a permanent magnet.

Protons and electrons of "soft" energies can be selectively recorded by analyzers having stopping and deflecting fields by appropriate choice of the polarity of the potential (or direction of the magnetic field). The effect of the background of high-energy particles is reduced by appropriate choice of the wall thickness of the body of the detection unit. Most often, the ratio of the flux of high-energy to low-energy particles is rather small.

However, whenever one is measuring any weak component of the particle flux, the problems of selective recording become serious, and special methods are

used to solve them. We can cite as an example a detector for determining deuterium in the solar wind (the D/H ratio is approximately 0.001).[56] The deuterium ions are accelerated in the detector to energies of 100 keV, and are focused on a tritium target. Nuclear reaction produces α particles of energies about 3.6 MeV. A semiconductor detector counts their number, which is proportional to the number of deuterium atoms.

We should note that the potential of the satellite (with respect to the surrounding plasma in the ionosphere) is usually very small (a fraction of an electron-volt), and it has no substantial effect on measurement of particles of energies above tens of eV. However, in some cases, in interplanetary space in particular, it can increase appreciably, and then we must no longer neglect it.

5. DETECTION OF NEUTRONS, γ-, AND X-RAY QUANTA

Thin scintillation counters are used most often to detect x-rays. The detectors are covered with a thin light-tight foil, made of beryllium as a rule. Beryllium foils are used because for γ and x-rays the probability of interaction of the radiation with matter depends on the atomic number Z of the matter as Z^5. Hence, beryllium, which has Z = 4, permits one to attain the least attenuation of the radiation (for equal film thicknesses) before it enters the sensitive volume of the detector. The thickness of the foil and the material (i.e., its Z value) set the lower energy limit of detectable quanta, while the thickness of the scintillator sets the upper energy limit. For example, on the Vela satellites[5] they used this type of scintillation counters having a CsI(Tl) crystal of thickness 5 mg/cm^2 covered with a beryllium foil 12 μ thick (2.3 mg/cm^2) or 25 μ thick (4.6 mg/cm^2). Thus they selectively recorded x-rays in the range 0.8—20 keV in the first case, and 2.5—20 keV in the second. The sizes of the fluxes to be measured by the detector lay within the range 6×10^3—6×10^7 keV/cm^{2}sec.

In order to measure increased x-ray flux densities, they used on the same satellites scintillating screens made of CsI. These converted x-rays into visible light, whose intensity was measured by a CdS photoelement. The detectors were protected from light by analogous beryllium foils.

Photon Geiger counters having thin windows made of aluminum or beryllium foils are also used as x-ray detectors.[57,58] In the described counters of this type, which were filled with an oxygen-neon mixture, the foil thickness was 2.7 mg/cm^2 of Al or 25 mg/cm^2 of Be. The detectors were installed on rockets and on the satellites Electron 2 and Electron 4, and measured energies in the ranges 0.6—1.5 keV and 1.2—6 keV.

Any x-ray detector unavoidably records also electrons that penetrate the filter and deposit a comparable energy in the scintillator. One can achieve selective detection most simply by measuring the radiation flux simultaneously with two detectors, one being sensitive to x-rays and the other relatively insensitive to x-ray quanta (e.g., a semiconductor electron detector). Then one works up the data obtained in the two detectors. One can conveniently use two analogous counters, but put an additional foil (gold or silver) in front of one of the counters to reduce considerably its efficiency for x-rays, while leaving its efficiency of recording electrons about the same.[58]

An effective measure for eliminating electrons is to put the detectors in a magnetic field, which prevents the electrons from entering the sensitive volume. For example, an ionization chamber having an aluminum foil 4 mg/cm^2 thick situated in a 2000-gauss magnetic field has been used to measure the flux density of x-ray quanta of several keV energy. Thus they prevented electrons of energy below 1 MeV from entering the detector.[59]

As a rule, scintillation detectors are used to detect γ-rays. They include scintillators of rather large dimensions (~50—100 cm^3). The lower energy limit of detectable quanta is determined by the thickness of the container, and usually amounts to 50—100 keV.

The fundamental problem that one must solve in detecting γ-quanta is to achieve selective recording on a background of charged-particle fluxes that occasionally rises to high values. The technique of layered phosphors is used most widely for rejecting charged particles. Here the crystal used to measure γ-rays is placed within a shield made of a scintillator differing in properties.[15,60-62] The inorganic crystals NaI(Tl) or CsI(Tl), made of high-density material, are usually used as the measuring crystal. The shields are made of plastic scintillators, which have an emission time 2—3 orders of magnitude shorter. An electronic circuit selects only those events when the main scintillator fires, but scintillations do not occur in the shielding detector.

Separate recording of γ-quanta and charged particles can also be achieved by Geiger-counter systems.[63,64] The main counter is surrounded by a ring of shielding counters connected with the main detector in an anticoincidence circuit. Only those events are recorded when the main detector fires, but none of the counters of the shielding ring do so.

The main problem in detecting neutrons is also how to attain high selectivity on a background of fluxes of charged particles and bremsstrahlung due to electrons. Hence, neutron detectors are used in space studies in which the amplitudes of signals due to detecting neutrons and other particles or quanta differ considerably. These detectors include boron and helium proportional counters and lithium scintillation counters.

Proportional counters filled with boron (enriched in the isotope B^{10}) or helium (the isotope He^3) are designed for detecting slow neutrons, and are usually used with moderators. In the nuclear reactions

$$He^3 + n \rightarrow p + H^3 + 0.77 \text{ MeV} \quad \text{and} \quad B^{10} + n \rightarrow Li^7 + \alpha + 2.78 \text{ MeV}$$

considerable energy is liberated, and is spent in ionizing the gas filling the counter. Electrons and soft photons are absorbed in the moderator. Relativistic protons are characterized by specific ionization losses that are too low (~2 keV/(mg/cm^2)). Thus the energy losses due to ionizing the gas per 2—3 cm pathway do not exceed 10 keV. Hence the neutron-detection events can be distinguished in the output of the proportional counter from events recording other particles or quanta in terms of the signal amplitude.

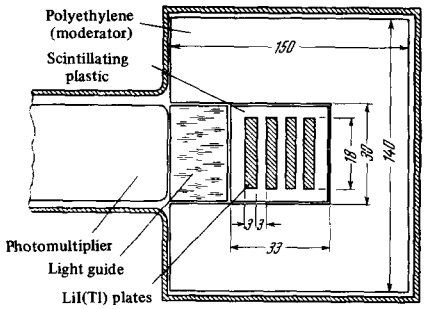

FIG. 11. Design of a scintillating neutron detector.

Helium proportional counters containing a polyethylene moderator were used on the Vela satellites.[5] Counters filled with BF_3 have been used in a number of satellites (e.g.[13,65]). The boron counters were placed in a paraffin moderator. Use of cadmium shields (~0.7 mm thick) in front of the moderator made it possible to reject slow neutrons (of energies below 0.5 eV).

When a flux of protons is acting on the counter, there is a certain probability of finding protons that have lost a certain fraction of their energy in the moderator and the walls of the counter, and then enter the gas filling the counter when "spent." This creates a background indistinguishable in its signal parameters from counting of neutrons. To eliminate this background (subtract it from the measured results), one uses two analogous counters having different counting efficiencies for neutrons. Thus, for example, two BF_3-filled counters have been used, one enriched to 96% in the isotope B^{10}, and the other to 12%. The ratio of neutron-counting efficiencies was eight, while the counting efficiencies for charged particles and quanta were identical.[13]

The most frequently used scintillation counters are detectors containing an LiI(Eu) crystal (e.g.[65]). In the reaction $Li^6 + n \rightarrow H^3 + \alpha + 4.76$ MeV, neutrons produce heavy particles having a high specific ionization. In order to identify neutrons and prevent charged particles from counting, one usually uses the layered-phosphor technique. The LiI(Eu) crystal is placed in a shield made of a scintillating plastic (Fig. 11). Passage of charged particles is accompanied by scintillations in the plastic scintillator, while as a rule, only the LiI scintillates when detecting neutrons. The considerable difference in emission times ($\tau_{LiI} \cong 2.2$ μsec, $\tau_{plast} \simeq 0.05$ μsec) permits one to distinguish signals coming from neutrons and charged particles from the shape of the current pulses.

In order to reduce the background due to γ-radiation (bremsstrahlung), the phosphor is designed in the form of alternating thin plates of LiI(Eu) and plastic scintillator. The range of the particles formed in the nuclear reaction is small, and as a rule is contained within an LiI plate. When γ-quanta are being detected, the electrons formed emerge from the LiI and enter the plastic scintillator.

Scintillating neutron counters have also been described[66] in which the detector is a liquid scintillator located within a shield made of a plastic scintillator.

The counter made use of pulse-shape discrimination (distinction of signals due to neutrons and charged particles).

6. DESIGN OF DATA-PROCESSORS AND ANALYZING INSTRUMENTS

Among the units contained in apparatus for measuring ionizing radiations besides the detectors, the design of data-processors and analyzing instruments is of interest. The factors most influencing the structure of these units are the features arising from the specifics of the object of measurement (in addition to general distinguishing features of units: economy, small dimensions, etc.).

As we have noted, charged particles in the intermediate- and high-energy range, and also γ and neutron fluxes, are measured with discrete detectors as a rule. For most of them (scintillation, proportional, and semiconductor counters), the energy distribution of the flux is established by pulse-height analysis of the output signals. Since the energy spectra are monotonic, the energy range is limited in most cases to one measurable by one type of detector, and since it is difficult to transmit a large volume of data by telemetric channels, a small number of energy channels is called for. Usually they have been chosen to be from four to eight in number (e.g.[25,28,67-69]). As a rule, the set of data is taken in parallel in all channels.

A typical pulse-height analysis instrument of this type includes a series of integral threshold stages linked to an anticoincidence selection circuit. The design of the analyzers handling the signals from the counters in telescopes is analogous.[20]

Numbers of channels above ten are used more seldom, but cases are known in which analyzers having 16 or more channels have been used in space studies. Most often, such multichannel analyzers are designed with a non-integrating-type memory. That is, the result of measuring the amplitude of each signal is held in coded form in the general memory unit of the satellite or of an earth-based instrument (after being transmitted through the communications channel), while data reduction is performed after the experiment is over. The data are recorded in binary code; instruments are known with 32- and 128-channel analyzers of this type,[70] and analyzers having 256[71,72] and 1500 channels.[73]

A merit of this way of designing the analyzer is that it considerably reduces the amount of apparatus to be installed on the satellite to take part in the experiment, with consequent simplicity and reliability of the instruments. Furthermore, the record permits one to reconstruct the dynamics of data accumulation. However, with this type of apparatus, the dead time after processing a unit event is determined by the characteristics of the memory unit of the space ship or the parameters of the communications channel. For example, a 1500-channel analyzer of this type[73] consumes a power of one watt, weighs 0.4 kg, and operates over the temperature range $-80° - +80°$C; the dead time amounts to 1 msec per event.

At the same time, several analyzers have been described having an internal memory built of ferrite cores. Such analyzers have been designed for 256 channels[74] ($T = -15° - +70°$C, $\tau_p = 26$ ms) and for 32 channels[15,75] (installed on the satellite Explorer XII and the space ship Ranger).

The design of analyzers for low-energy charged particles is more specific. Analyzers both with stopping

and with deflecting fields are usually designed for stepwise scanning of the energy spectrum with one recording channel. This considerably impairs the time characteristics of the apparatus. The entire energy spectrum is usually scanned with a series of discrete values of the stopping or deflecting field (from 4 to 16). Often the voltage is not increased linearly, but more sharply, so as to ensure constancy of the ratio of the channel width to the energy (see, e.g.[38,40,47]). However, in some instruments, e.g., on the Vela satellites,[5] the number of energy steps was raised to 64.

Stepwise analysis makes for added difficulties, even with slow-action telemetry, since arbitrary reference to the data-processors becomes inadmissible. Here the results of measurements corresponding to each level of the stopping or deflecting field are recorded in their own memory channel. As new data are collected, they take the place of those stored earlier.[76]

The fundamental problems in designing data-processors involve the wide range of the values to be measured and the restriction on the data that can be transmitted by telemetric channels.

Among the discrete-signal processors following directly after the detectors, or after selection or analysis stages, the most common are scalers, or ratemeters when the pulse rates are high.

Among the ratemeters, the logarithmic units cover a rather wide range of rates when the data is transmitted on a single channel. The instruments most stable in operation are those designed according to the principle of adding currents from a series of diode integrators having different parameters (see, e.g.[58,77]). They cover rates from several pulses/sec to $(10-20) \times 10^3$ pulses/sec. However, the error is as much as 20% of the increment in the readings per tenfold increase in the signal rate.

One can gain an increase in accuracy of measurement in ratemeters with linear, automatically-switched subranges.[78] The data are transmitted on two channels: one channel transmits the readings directly, and the other transmits the subrange code.

In counting circuits, there are no limitations in principle on the width of the range of rates of the signals being measured. Only the number of bits whose state must be interpolated increases as the range is broadened. For example, when the required accuracy is 10% and the dynamic range is 10^5, one needs a size of counting circuit subject to interpolation of no less than 10^6 (i.e., 20 bits). Thus, the fundamental difficulty in using counting circuits arises in output of the readings. Usually data on the state of three (rarely four) flip-flops are output on one channel. When each flip-flop goes over to the state "1," it sends to the interpolator a current having a value accounting for the weight of the flip-flop in the circuit, and increasing sequentially by a factor of two in the chain of flip-flops (see, e.g.[64,79,80]).

A highest-significant-bit interpolator[81] is used to transmit on one channel data on the state of the many flip-flops in the counting circuit. In such an interpolator, each of the flip-flops controls one of the switching transistors (the triode becomes saturated when the flip-flop fires). The collectors of the transistors are connected through resistors whose values are selected to make the readings from the interpolator proportional to the order number of the highest of the flip-flops that have fired. Such an apparatus is rather simple, and permits transmission of data on a single channel. However, the mean error is close to 25%. Greater accuracy can be gained when a second channel transmits the state of several of the lower bits following directly after the highest bit, while the one channel transmits the order number of the first significant bit. When data on the state of four or five subsequent bits is transmitted, the error is reduced to 1.5% or to 0.75%. Two types of such systems have been described. In the one type, the flip-flops are interrogated after the measurement is finished, and in the other the data reduction is performed during the counting process.[81-83]

Finally, in order to reduce the volume of data to be transmitted from the counting system, one can use continuous indication of the states of several flip-flops alone, uniformly selected out of the total number of cells.[84] The mean rate is determined from the time intervals between changes of state of the flip-flops. When the rate is low, it is determined from the period of alternation of one of the first flip-flops of the system, but from the period of alternation of the last flip-flop if the rate is large.

The states of several flip-flops can be transmitted on a single channel in an amplitude code. The rate of variation of the mean signal frequency is limited in such systems; there must be no substantial changes within the time that it takes a flip-flop to transform from one state to the other, lest the change of state of the preceding flip-flop to be interpolated occur too often, and not be decoded.

When measuring the current in the collector circuit of detection units for low-energy particles, the problem of covering a broad range is also very serious. Solution of the problem is complicated also by the fact that the currents to be measured are themselves rather small: from 10^{-13} A (or 10^{-14} A) to $10^{-6}-10^{-5}$ A.

In order to extend the dynamic range of measurements by direct-current amplifiers, a logarithmic conversion element (vacuum diodes or pentodes, and also semiconductor devices) is introduced into the amplifier.

Vacuum diodes are usually used in a negative-feedback circuit of the amplifier, and they permit one to cover a range of measurements of six or seven orders of magnitude, starting with $10^{-10}-10^{-11}$ A.[85] The fundamental difficulties in using such a logarithmic element involve the small drop in voltage as the current increases by an order of magnitude (~0.2 V) and the considerable drift in the output voltage (~0.1 V after several hours of operation).

Semiconductor diodes or transistors in the negative-feedback circuit[86] are only used for currents in the end region of the measured range ($10^{-7}-10^{-6}$ A). Semiconductor devices are sensitive to temperature variation and show an even smaller voltage drop as the current being measured increases by an order of magnitude; these are the practical difficulties encountered in designing circuits.

Finally, a logarithmic amplifier has been designed using an economical directly-heated pentode as the leading element. The tube operated in a grid-current system ($i_{in} = i_g$), while the voltage on the shield of the negative-feedback system was varied so as to keep the anode

current invariant. Here the shield potential turns out to be proportional to the logarithm of the input current.

Currents have been measured by similar circuits over the range from 10^{-14} to 10^{-7} A. However, they are characterized by considerable error of measurement, mainly due to drift in the direct-current amplifier, and becoming as much as 15–20% of the voltage drop for an increase in the current by an order of magnitude. Furthermore, one can apply these systems only to measure direct current of positive polarity.

In order to improve the accuracy and obtain a broad dynamic range of direct-current measurements, a number of instruments have used analog-digital converters. The simplest instrument of this type consists of a circuit that charges a capacitor that is then discharged through a neon lamp when the voltage on the capacitor attains the firing potential.[88] Owing to the large voltage drop $U_{firing} - U_{glow}$ and the relatively large capacities, the measurable currents are above 10^{-9} A, and the system can be applied only for operation with a photomultiplier, secondary-electron multiplier, etc.

One can get high sensitivity in stages based on electrometric direct-current amplifiers. Here, the current to be measured charges a capacitor in the feedback circuit, which is discharged by pulses imparting a calibrated amount of electricity. The described instruments of this type[89] have measured currents over the range from 10^{-12} to 10^{-6} A with an accuracy of ±1%.

Relay instruments have also been used for amplitude-digital conversion. Thus, in one of these processors,[90] the current to be measured charged a capacitor for a fixed time. Then the capacitor was discharged into an inductance through the contacts of a relay. The voltage appearing in the oscillation contour was amplified and subjected to pulse-height analysis. The number of oscillation periods having an amplitude lying above a fixed level was recorded. The exponential decay of the oscillations permits one to get directly the logarithmic calculating characteristic of the stage.

One must also provide for a logarithmic measuring characteristic in recording the modulated current in selectors of low-energy charged particles. This is done by using various non-linear elements: semiconductor diodes, transistors, etc.

As the program of experiments is expanded and the volume of information obtainable in them increases, the problem of condensing the information on board the space ship gains in importance. This poses the problem of designing processors that work up the incoming information, and transmit to Earth the data of greatest interest. This considerably increases the efficacy of processing of the data of the measurements, and improves the efficiency of use of the telemetric communications channels, which usually limit the volume of information that can be transmitted.

Thus, for example, rather than the points of spectral distributions, angular distributions, etc., one can transmit in a channel the parameters of these distributions derived on board the space ship (the value of the parameter at the peak of the distribution, the dispersion, the current density at the peak, etc.). However, such a design of the apparatus involves considerable complication, and requires a marked increase in the reliability of operation of the electronic elements and units. Apparently, introduction of integrated circuits into apparatus to measure radiation will permit solution of these problems, and progress toward a more extensive treatment of information on board the space ship.

We should emphasize the great dynamism of the branch of technology involved with inventing apparatus for space studies. In designing apparatus, scientists continually try to take into account the results of experiments already performed, and steadily to improve devices and instruments. We have given in this review data on apparatus for measuring radiation invented less than ten years ago. Undoubtedly, refinement of methods and apparatus will permit us in the immediate future to obtain a more detailed and reliable picture of the fluxes of ionizing radiation in the Earth's vicinity and in outer space. In this review we haven't discussed a number of specific problems of great interest in designing apparatus. For instance, they include problems of calibrating and testing the characteristics of detectors, both before launching a satellite and while it is in flight. However, this comprises a separate major topic.

In conclusion, the authors of this review express deep gratitude to Yu. I. Gal'perin for discussion of the problems discussed in the review, and for aid rendered in writing it.

[1] Space Physics, Ed. D. P. Le Galley and A. Rosen, Wiley, 1964.

[2] E. N. Parker, Scient. American 210 (4), 66 (1964).

[3] J. I. Vette, IEEE Trans. NS-12, No. 5, 1 (1965).

[4] B. J. O'Brien, Interrelations of Energetic Charged Particles in the Magnetosphere, Dept. of Space Science, Rice Univ., Texas, 1966.

[5] S. Singer, Proc. IEEE 53, 1935 (1965).

[6] B. J. O'Brien, Science 148, 449 (1965); Russ. transl., Usp. Fiz. Nauk 89, 681 (1966).

[7] L. J. Cahill, Sci. American 212, No. 3, 58 (1965); Science 147, 991 (1965); Russ. transl., Usp. Fiz. Nauk 87, 539, 551 (1965).

[8] S. N. Vernov, in collected volume Issledovaniya kosmicheskogo prostranstva (Space Studies), M., "Nauka", 1965, p. 277.

[9] A. Konradi, J. Geophys. Res. 71, 2317 (1966).

[10] S.-I. Akasofu, Sci. American 213, No. 6, 55 (1965); Russ. transl., Usp. Fiz. Nauk 89, 669 (1966).

[11] V. G. Bobkov et al., Radiatsionnaya bezopasnost' pri kosmicheskikh poletakh (Radiation Safety in Space Flights), M., Atomizdat, 1964.

[12] D. K. Bailey, J. Geophys. Res. 67, 391 (1962).

[13] J. P. Martin, ibid. 70, 2057 (1965).

[14] S. Hayakawa, Space Res., Vol. 3, North-Holland Publ. Co., Amsterdam, 1963, p. 984.

[15] A. E. Metzger et al., Nature 204, 766 (1964).

[16] A. A. Kmito, Metody issledovaniya atmosfery s ispol'zovaniem raket i sputnikov (Methods of Atmosphere Study Using Rockets and Satellites), L., Gidrometeoizdat, 1966.

[17] J. H. Rowland, J. C. Bakke, W. L. Imhof and R. V. Smith, IEEE Trans. NS-10, No. 1, 178 (1963).

[18] F. S. Mozer, D. D. Elliott, J. D. Mihalov, G. A. Paulikas, A. L. Vampola, and S. C. Freden, J. Geophys. Res. 68, 641 (1963).

[19] J. B. Reagan and R. V. Smith, IEEE Trans. NS-10,

No. 1, 172 (1963).
[20] I. A. Savenko, O. I. Savun, and A. V. Yurovskiĭ, Geomagnetizm i aéronomiya 5, 550 (1965); Geomagnetism and Aeronomy 5, 423 (1965).
[21] S. N. Vernov et al., see Ref. 8, p. 394.
[22] B. O'Brien et al., in collected volume Radiatsionnye poyasa Zemli (Radiation Belts of the Earth), M., IL, 1962, p. 72.
[23] G. S. Dragun et al., in collected volume Iskusstvennye sputniki Zemli (Artificial Earth Satellites), No. 9, M., AN SSSR, 1961, p. 87.
[24] Ya. L. Blokh et al., see Ref. 8, p. 514.
[25] I. A. Savenko, O. I. Savun, P. I. Shavrin, and B. M. Yakovlev, Geomagnetizm i Aéronomiya 5, 546 (1965); Geomagnetism and Aeronomy 5, 420 (1965).
[26] J. A. Simpson and J. J. O'Gallagher, Wescon. Tech. Paper., Pt. 5, 1965, p. 4.
[27] L. Koch and J. F. Crifo, Onde l'electr. 43, 325 (1963).
[28] R. W. Fillius and C. E. McIlwain, see Ref. 14, p. 1122.
[29] R. A. Cail, G. E. C. Journal 32, 98 (1965).
[30] B. Wolfe, A. Silverman, and J. W. DeWire, Rev. Sci. Instr. 26, 504 (1955).
[31] L. Wählin, Nuclear Instr. and Methods 14, 281 (1961).
[32] H. E. Hinteregger, J. Geophys. Res. 66, 2367 (1961).
[33] K. I. Gringauz et al., DAN SSSR 131, 1301 (1960); [Sov. Phys.-Doklady 5, 361 (1960)].
[34] K. I. Gringauz, see Ref. 23, No. 12, 1962, pp. 105 and 119.
[35] Yu. I. Gal'perin and V. I. Krasovskiĭ, Kosmicheskie Issledovaniya 1, 126 (1963).
[36] N. V. Dzhordzhio, Geomagnetizm i Aéronomiya 6, 424 (1966); [Geomagnetism and Aeronomy 6, 339 (1966)].
[37] H. S. Bridge, C. Dilworth, B. Rossi, F. Scherb, and E. F. Lyon, J. Geophys. Res. 65, 3053 (1960).
[38] H. S. Bridge, A. J. Lazarus, E. F. Lyon, B. Rossi, and F. Scherb, see Ref. 28, p. 1113.
[39] A. Bonetti, et al., J. Geophys. Res. 68, 4017 (1963).
[40] S. N. Vernov et al., see Ref. 8, p. 381.
[41] M. Bader, J. Geophys. Res. 67, 5007 (1962).
[42] V. V. Mel'nikov, I. A. Savenko, B. I. Savin, and P. I. Shavrin, Geomagnetizm i Aéronomiya 5, 148 (1965) [Geomagnetism and Aeronomy 5, 107 (1965)].
[43] I. A. Savenko, B. I. Savin, V. V. Mel'nikov, P. I. Shavrin, and T. N. Markelova, Geomagnetizm i Aéronomiya 5, 749 (1965) [Geomagnetism and Aeronomy 5, 579 (1965)].
[44] B. Hultqwist, Proc. Symp. on High Latitude Particles and the Ionosphere, Alpbach, 1964, London, Logos Press Book, 1964, p. 153.
[45] R. L. F. Boyd, ibid., p. 1.
[46] B. I. Savin, Geomagnetizm i Aéronomiya 1, 995 (1961) [Geomagnetism and Aeronomy 1, 863 (1961)].
[47] C. W. Snyder and M. Neugebauer, see Ref. 14, Vol. 4, p. 89, 1964.
[48] G. Skovli, see Ref. 44, p. 147.
[49] M. Bader, see Ref. 14, Vol. 3, p. 358, 1963.
[50] V. I. Krasovskiĭ, Yu. I. Gal'perin, V. V. Temnyĭ, T. M. Mulyarchik, N. V. Dzhordzhio, M. Ya. Marov, A. D. Bolyunova, O. L. Vaĭsberg, B. P. Potapov, and M. L. Bragin, Geomagnetizm i Aéronomiya 3, 401 (1963) [Geomagnetism and Aeronomy 3, 333 (1963)].
[51] R. D. Sharp, J. B. Reagan, S. R. Salisbury, and L. F. Smith, J. Geophys. Res. 70, 2119 (1965).
[52] H. M. Gibbs and E. D. Commins, Rev. Sci. Instr. 37, 1385 (1966).
[53] K. W. Ogilvie et al., Compt. rend. 6-e Conf. Internat. Phenomenes Ionisat. Gaz., Vol. 4, Paris, 1963, p. 91.
[54] D. L. Lind and N. McIlwraith, IEEE Trans. NS-13, No. 1, 511 (1966).
[55] H. E. Hinteregger, L. A. Hall, and W. Schweirer, Astrophys. J. 140, 319 (1964).
[56] F. W. Floyd and F. Scherb, IEEE Trans. NS-13, No. 2, 18 (1966).
[57] I. P. Tindo and A. I. Shurygin, Kosmicheskie Issledovaniye 3, 262 (1965).
[58] B. N. Vasil'ev, ibid. 4, 748 (1966).
[59] L. W. Acton et al., J. Geophys. Res. 68, 3335 (1963).
[60] J. R. Arnold, A. E. Metzger, E. C. Anderson, and M. A. Van Dilla, ibid. 67, 4878 (1962).
[61] D. Schwartz and L. E. Peterson, Trans. Amer. Geophys. Union 46, 129 (1965).
[62] M. A. Van Dilla et al., Trans. IEEE NS-9, 405 (1962).
[63] S. I. Fan, R. Mayer, and I. A. Simpson, see Ref. 22, p. 85.
[64] S. I. Avdyushin, N. K. Pereyaslova, and N. E. Petrenko, see Ref. 8, p. 511.
[65] S. J. Bame, J. P. Conner, F. B. Brumley, R. L. Hostetler, and A. C. Green, J. Geophys. Res. 68, 1221 (1963).
[66] R. B. Mendell and S. A. Korff, ibid. 68, 5487 (1963).
[67] D. B. Hicks, L. Ried, Jr., and L. E. Peterson, IEEE Trans. NS-12, No. 1, 54 (1965).
[68] J. H. McQuaid, IEEE Trans. NS-13, No. 1, 515 (1966).
[69] J. R. Marbach, IEEE Trans. NS-13, No. 1, 464 (1966).
[70] C. J. Ewald and A. A. Sarkady, IEEE Trans. NS-13, 537 (1966).
[71] S. Way et al., ibid., p. 523.
[72] C. E. McIlwain, J. Geophys. Res. 65, 2727 (1960).
[73] J. T. A. Ely, IEEE Trans. NS-13, No. 1, 533 (1966).
[74] R. M. Rodrigues, IEEE Trans. NS-12, No. 1, 66 (1965).
[75] D. A. Bryant, T. L. Cline, U. D. Desai, and F. B. McDonald, J. Geophys. Res. 67, 4983 (1962).
[76] A. J. Lazarus, H. S. Bridge, and J. Davis, ibid. 71, 3787 (1966).
[77] S. I. Babichenko et al., Kosmicheskie Issledovaniya 3, 237 (1965).
[78] S. Thomas, IEEE Trans. NS-10, No. 1, 36 (1963).
[79] G. S. Dragun et al., see Ref. 23, No. 9, p. 86.
[80] B. N. Vasil'ev et al., see Ref. 23, No. 15, p. 83.
[81] L. S. Gorn and B. I. Khazanov, Registratory intensivnosti izlucheniĭ (Radiation Intensity Recorders), M., Atomizdat, 1965, pp. 238–240.
[82] I. D. Ivanov and B. I. Khazanov, in collected volume Trudy VI nauchnotekhnicheskoĭ konferentsii po yadernoĭ radioélektronike (Proceedings of the 6th Scientific-Technical Conference on Nuclear Radioelectronics), Vol. I, M., Atomizdat, p. 133.
[83] S. N. Vernov et al., see Ref. 8, p. 394.
[84] C. S. Josias, Proc. IRE 48, 415 (1960).
[85] S. K. Chao, Rev. Sci. Instr. 30, 1087 (1957).
[86] W. L. Paterson, Rev. Sci. Instr. 34, 1311 (1963).

[87]S. R. Bishop, IEEE Trans. **NS-13**, No. 1, 602 (1966).
[88]P. V. Vakulov, N. N. Goryunov, Yu. I. Logachev, and E. N. Sosnovets, Geomagnetizm i Aéronomiya 1, 880 (1961) [Geomagnetism and Aeronomy 1, 767 (1961)].
[89]H. Doong, IEEE Trans. **NS-12**, No. 4, 370 (1965).
[90]Yu. V. Mineev, A. A. Sanin, B. I. Savin and A. N. Gadalov, Geomagnetizm i Aéronomiya 5, 781 (1965) [Geomagnetism and Aeronomy 5, 608 (1965)].

Translated by M. V. King